Temporal wavefront stability of an ultrafast high-power laser beam

Juan M. Bueno,[1,*] Brian Vohnsen,[1,†] Luis Roso,[2] and Pablo Artal[1]

[1]Laboratorio de Óptica, Centro de Investigación en Óptica y Nanofísica (CiOyN), Universidad de Murcia, Campus de Espinardo, 30100 Murcia, Spain

[2]Servicio Láser, Universidad de Salamanca, 37008 Salamanca, Spain

*Corresponding author: bueno@um.es

Received 5 September 2008; revised 18 December 2008; accepted 19 December 2008; posted 5 January 2009 (Doc. ID 101030); published 26 January 2009

We measured the temporal dynamics of wavefront aberrations in a beam produced by a commercial ultrafast high-power laser with a research-prototype real-time Hartmann–Shack wavefront sensor. Measurements were performed at two different temporal rates for a 7 mm diameter. Results showed that changes in the wavefront aberrations were always lower than 1%. The main contribution to the total root-mean-square (RMS) wavefront error was due to the effects of low order aberrations (defocus and astigmatism), which persisted even after cavity realignment. The potential improvement in the beam quality after correction of the different aberration modes was also shown. Real-time measurements of laser aberrations while modifying cavity parameters might be a useful tool to improve the beam quality.

OCIS codes: 140.0140, 010.7350, 220.1010, 320.7090.

1. Introduction

Many experiments in laser-matter interaction require high-intensity and high-quality stable focusing. In particular, most of the strong field laser-atom interaction effects depend on the ability to focus the beam into a very small volume, and this requires a high-quality beam profile. However, wavefront aberrations (WAs) present in the beam enlarge the focal spot size and may reduce the power density dramatically. Moreover, WAs can also change the temporal profile of the pulse.

In ultrafast (femtosecond) high-power lasers, some aberrations result from imperfections and misalignments of the internal optical components mainly located in the amplification chain (such as lenses, mirrors, polarizers, or beam splitters) [1,2]. These are relatively stable aberrations over long temporal periods (static). Moreover there is another type of aberrations named thermo-optical (dynamic or pump-shot) aberrations. These arise during the strong heat generation within the optical pumping [1–4]. At high intensities, those effects can be amplified by the nonlinear response of the interaction. Other factors such as vibrations, the amplifiers' cooling-down process, room-temperature, draught, or non-air disturbance might also affect the laser stability and modify the WAs of the beam.

During the last decade much effort has been devoted to measure the WAs of high-power lasers and to improve the beam quality. Both static aberrations and thermally induced optical distortions in the active medium are key issues that have to be overcome when laser efficiency needs to be optimized. Some authors used wavefront sensing techniques [3–7], although alternative methods have also been reported: random phase plates, spatial and temporal coherence reduction, shearing interferometry, or phase-retrieval methods [8–13].

Accurate knowledge of the laser beam wavefront is the first step towards producing highly-focused homogeneous intensity spots. If the beam WA is determined, the distorted intensity pattern in the focal

0003-6935/09/040770-08$15.00/0

spot can be predicted and, thus, the subsequent benefit of using adaptive optics for the WA correction can be specified. High-power lasers are dynamic optical systems and the WA of the emergent beam might suffer fluctuations at different temporal rates [14]. Therefore, a reliable and fast instrument is required for an accurate pulse wavefront measurement.

A number of experiments reported data of WAs within the cavity of high-power laser systems [1,15–18]. These are typically not commercially-available prototypes. Moreover, many of the optical elements are customized to be suitable for these devices. Only a few provided WA measurements out of the amplification chain [5–7].

In this work we investigate the WA stability of a laser beam provided by a commercially-available high-power laser system. Measurements have been carried out with a Hartmann–Shack (HS) wavefront sensor [19,20] placed at the output of the laser system.

2. Experimental System and Procedure

To measure the WA of the high-power laser we built a HS sensor using commercial off-the-shelf elements. This type of sensor is particularly well suited for this type of laser. We used an amplified Ti:sapphire laser [Legend, Coherent, St. Clara, California] with 1 kHz repetition rate 130 fs pulse width and peak powers of up to 10 GW. The experimental setup is illustrated in Fig. 1. The horizontally polarized high-power emergent laser beam ($\lambda = 797$ nm, ~600 mW) is incident onto an optical window at approximately its Brewster angle (φ_B), and the reflected power of the beam is reduced up to 10^{-3}. The sampled beam containing this small fraction of power is used for the wavefront sensing. It passes through a variable aperture (AP) used to set the size of the beam to the desired diameter. A set of metallic neutral density filters (NDF) avoids the damage of the HS wavefront sensor which is composed of a microlens array (ML, aperture size of 0.6 mm) and a CCD camera. The CCD is able to acquire images a rate of 25 Hz that are viewable directly on a monitor. Both registration and image processing were done using in-house developed software. A typical HS spot pattern obtained with our instrument is shown in the inset included in Fig. 1.

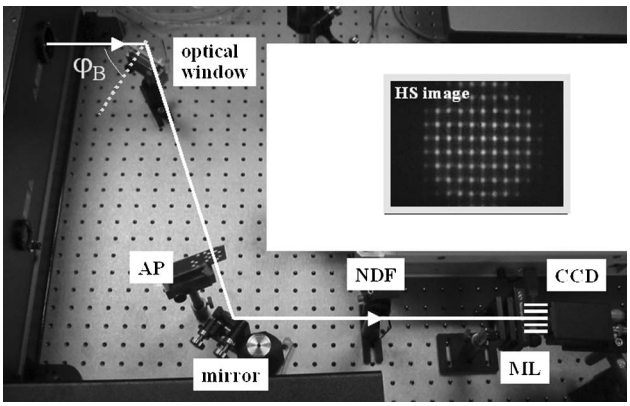

Fig. 1. Hartmann–Shack wavefront sensor used to measure the wavefront aberration stability of a high-power laser beam.

The WA of the laser beam was computed for each registered HS image [21,22]. Briefly, if the wavefront of the laser beam reaching the ML is plane, the CCD records an image containing a perfectly regular mosaic of spots as determined by the array of microlenses. However, if the wavefront is aberrated (i.e., distorted) the pattern of spots is irregular. The displacement of each spot is proportional to the derivative of the wavefront over each microlens area. From each HS image, the WA of the laser beam is calculated and expressed as a Zernike polynomial expansion up to 6th order over a 7 mm pupil. The number of microlenses (i.e., HS spots) within the pupil size we used allows for accurate measurement of WAs. The root-mean-square (RMS) as well as the peak-to-valley value (PtV) were used as quality parameters. For the far-field point spread functions (PSFs) computed from the WAs, the parameter we used was the Strehl ratio. This was defined as the ratio between the volumen of the MTF computed from the actual PSF and the corresponding volume for the difraction-limited MTF for the same pupil size.

The experimental procedure was split into two parts. In the first one, HS images were registered at two different temporal rates during several hours. These rates were 25 and 10^{-3} Hz, respectively. In the second part, similar measurements (i.e., same temporal rates) were carried out three months later (also during a unique experimental session), after the laser power was optimized and the optics inside the cavity cleaned and realigned.

3. Results

Figure 2 shows the WAs (from 2nd to 6th order) and the corresponding calculated PSFs (i.e., the far-field intensity distribution) for four images registered at different temporal intervals (0 s, 500 ms, 15 min, and 1 h). Both WAs and the corresponding calculated PSFs remained quite stable over time.

Figure 3 shows the values of total RMS for the WAs computed at two temporal rates. Data of the plot on the left are those computed from HS images registered at 25 Hz during 1 s (once every 40 ms). The plot

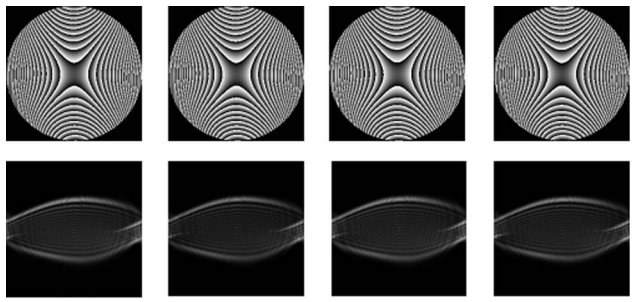

Fig. 2. WAs (2π phase wrapped, 7 mm pupil) including Zernike terms from 2nd to 6th order computed from HS images registered at 0 ms, 500 ms, 15 min, and 1 h (upper row), and the corresponding calculated far-field PSFs (bottom row). PSFs subtend 1.7°.

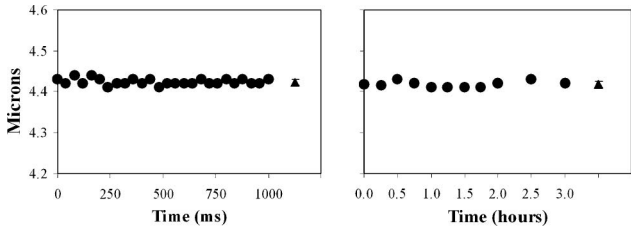

Fig. 3. RMS values for the WAs computed from HS images registered at two different temporal rates: 25 Hz during 1 s (left) and 0.001 Hz during 3 h (right). The triangles correspond to the mean. The error bars are the standard deviation (they are almost within the symbol).

on the right corresponds to images registered at 10^{-3} Hz during 3 h (i.e., one image every 15 min). For the former the differences between the maximum and the minimum values were 0.03 μm, which correspond to 0.68%. These differences were 0.02 for the latter (0.45%). These results show that the overall measured WA was stable over time. The temporal stability of the high-power laser beam WA can also be checked when analyzing the results for PtV values (not shown in the figure). Maximum differences were 0.38 and 0.37 μm, respectively, for both temporal rates (~1.46%).

The qualitative shape of the WA indicates that there is a large influence of low order aberrations. To explore this, the values of the Zernike coeficients (up to 4th order) of the WA corresponding to one HS image (1 frame) are depicted in Fig. 4. For comparison we have also included the averaged values for 1 s and 3 h. The temporal stability in the individual Zernike terms corroborates the results of previous figures. Moreover the plot also shows that defocus (Z_2^0) and horizontal–vertical (H-V) astigmatism (Z_2^2) are the dominant aberrations (~95% of the total RMS value). The former is responsible for the spatial divergence (or convergence) of the laser beam. For every Zernike term beyond 2nd order, the mean value was lower than 0.05 μm except for the terms Z_3^{-3} (trefoil, mean: –0.091 μm) and Z_4^0 (spherical aberration, mean: 0.131 μm).

Figure 5 shows the RMS values when excluding defocus and astigmatism terms for the same temporal scales as in Fig. 3. The maximum difference in RMS values was also similar during 1 s and 3 h. Changes in defocus and astigmatism themselves during 1 s and 3 h are depicted in Fig. 6. The maximum changes during 3 h were 0.025 μm for defocus and 0.007 μm for astigmatism.

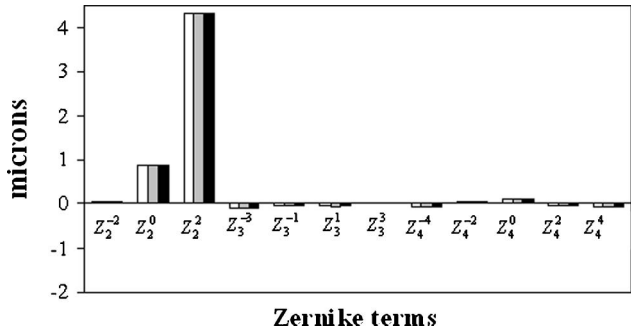

Fig. 4. Individual Zernike coefficient values of the WA (up to 4th order) for the high-power laser beam. Data correspond to one frame (white bars) and the average during 1 s (gray bars) and 3 h (black bars).

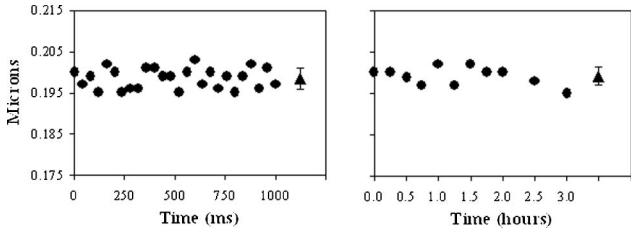

Fig. 5. RMS values (excluding defocus and astigmatism) for the WAs computed from HS images registered at the same temporal rates as those in Fig. 3. Triangles represent the mean and the error bars are the standard deviation.

As a final test to explore the laser WA stability, this was computed taking the first HS image as a reference (instead of using a plane wavefront reference). Figure 7 shows the results as a function of time. The "residual" RMS and PtV values ranged between 0.049 and 0.060 μm for the former and between 0.423 and 0.657 μm for the latter.

Three months after this first experiment, the optical elements inside the amplifier were realigned and cleaned to optimize the output power (~1 W). A new set of measurements was carried out for similar experimental conditions. Figure 8 presents the WAs and PSFs as a function of time when including all Zernike terms (apart from piston and tilts).

For these conditions the light beam WAs hardly changed with time (although they changed much compared to those obtained before cavity alignment). During 1 h the maximum differences in PtV and RMS values were 0.335 and 0.016 μm, respectively. However, if excluding defocus and astigmatism the differences were larger: 0.564 and 0.035 μm, respectively. Figure 9 depicts the RMS values of the WA of the

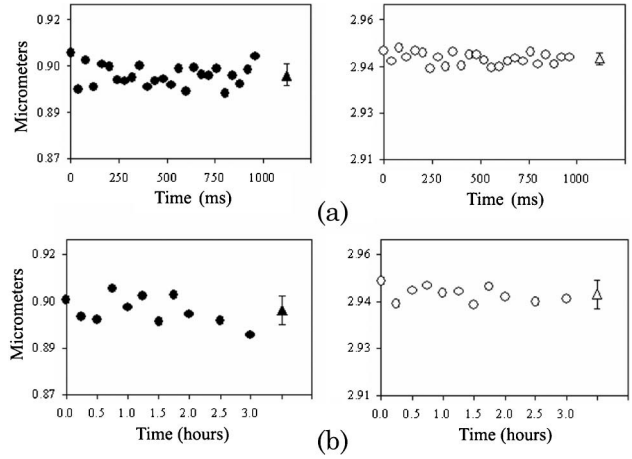

Fig. 6. Temporal evolution of the values of defocus (left plots) and astigmatism (right plots) terms for the two temporal scales: (a) 1 s and (b) 3 h. Triangles represent the averaged value.

Fig. 7. "Residual" WAs for the high-power laser beam using the first HS image (time = 0) as a reference. Left to right panels correspond to the time sets of 1 s, 15 min, 1 h, and 3 h.

high-power laser beam as a function of time. Despite the careful alignment of the internal laser optics, the 2nd order Zernike modes are still dominant.

Table 1 compares results before and after the cavity realignment. Overall the total RMS value decreased approximately to one half of the original value. This is due to a significant reduction in astigmatism. Conversely, when excluding 2nd order terms, the RMS value increased around 50% after the internal optics realignment. This means that this operation is a relevant factor in the laser beam WA affecting not only defocus and astigmatism but also higher-order aberrations.

The comparison of averaged individual Zernike terms after (white and gray bars) and before (black bars) the realignment is plotted in Fig. 10. The amount of astigmatism was noticeably reduced (see also Table 1) and the defocus term changed from a positive value to a negative one. Values for spherical aberration remained similar.

At this point we have explored the changes in the high-power laser beam WA with time. These aberrations were measured at the output of the laser and our experimental system is not able to detect the sources of the different terms. However, since these might be static and/or dynamic, any WA correction technique (i.e., deformable mirror, liquid crystal spatial light modulator) used to improve the laser focusability would have to take this into account. Figure 11 presents a numerical simulation where the benefit of using adaptive optics for wavefront correction is shown.

The WA on the left corner of Fig. 8 includes all Zernike terms from 2nd to 6th orders and is taken as a reference for WA correction (RMS_{WA} : 2.149 μm). Panels on the left of Fig. 11 present the results for both the WA and the PSF with defocus removed. Both noticeably improve, although some astigmatism remains in the PSF. The RMS value was 0.357 μm (PtV values reduced more than 50%). When eliminating the astigmatism terms (second column from the left), the RMS value was 0.312 μm (PtV value decreased ~15%). There is a moderate improvement since the PSF becomes more symmetric due to the absence of astigmatism. There is a slight improvement in the WA and PSF when eliminating the contribution of 3rd order terms (third column of panels, RMS_{WA} : 0.268 μm). When 4th order terms are not taken into account the PSF noticeably improves and the energy concentrates in a much smaller spot as the panel at the far right bottom corner shows (RMS_{WA} : 0.146 μm). Finally, Fig. 12 depicts the increase in Strehl ratio of the PSF when eliminating the different terms of the Zernike expansion.

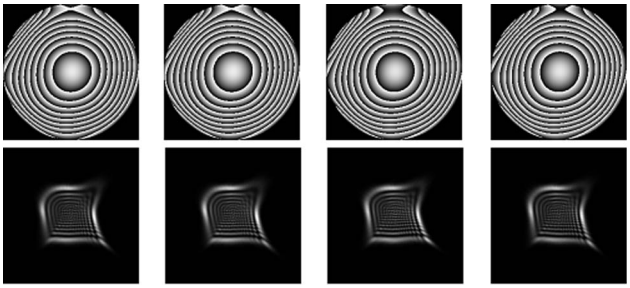

Fig. 8. WAs (upper row) and PSFs (bottom row) including Zernike terms from 2nd to 6th order as a function of time once the optics inside the laser system was realigned. From left to right: $t = 0$, 1 s, 15 min, and 1 h. All panels subtend the same as in Fig. 2.

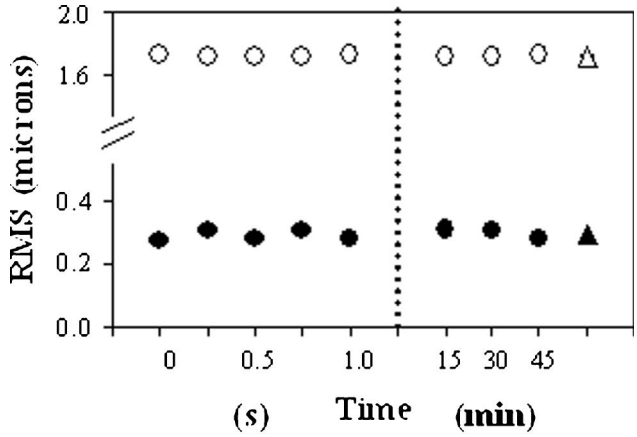

Fig. 9. Values of RMS for the laser beam WAs after the cavity realignment as a function of time: total RMS (white symbols) and RMS for 3rd order terms and higher (black symbols). Triangles represent the mean value. Error bars are within the symbols.

4. Discussion and Summary

We measured the WAs of an ultrafast high-power laser beam. This was performed by means of a custom-built HS sensor placed at the output of a commercially-available femtosecond laser system. Since WAs reduce the desired intensity of the laser pulse, which is required for a large variety of physics experiments, a complete characterization of a laser beam requires an analysis of the temporal dependence of the WA.

Here we have assessed the WAs for a 7 mm diameter pupil across the beam at two different temporal rates. We have found that the laser WA was quite stable over time (at least on the time scale of our HS sensor). Variations in total RMS (2nd order Zernike terms and higher) were similar for both temporal scales and they were never larger that 1% (Fig. 3). In terms of PtV, these were about 1.5%. These little temporal changes can also be qualitatively observed in both WAs and PSFs (Figs. 2 and 7).

The analysis of the Zernike terms shows that about 95% of the RMS wavefront error is contained within the 2nd order Zernike modes: primarily defocus and astigmatism. In terms of temporal changes,

Table 1. Values of RMS and Other Aberration Terms Before and After Realigning the Optics Inside the Laser Cavity

	Total RMS	RMS 3rd Order and Higher	Defocus	Astigmatism	Spherical
Before	4.43 ± 0.01	0.19 ± 0.00	0.90 ± 0.01	4.32 ± 0.01	0.13 ± 0.01
After	2.15 ± 0.01	0.29 ± 0.02	-2.12 ± 0.01	0.17 ± 0.01	0.13 ± 0.01

those associated with defocus are higher than those for astigmatism (1.45% and 0.24%, respectively).

After intracavity alignment, measurements for the same experimental conditions were repeated. Once again WAs presented little changes along the temporal rates they were measured (Figs. 8 and 9). Variations with time were similar to those found before realignment.

Despite that 2nd order Zernike terms remained dominant, laser beam WAs were clearly different before and after the cavity alignment (see Figs. 4 and 10). The total RMS value was dramatically reduced due to a significant decrease in astigmatism (see Table 1), however the defocus term changed from ~ 0.90 to $\sim -2.12\,\mu$m. On the other hand, the RMS values corresponding to 3rd order terms and higher increased. These changes are mainly due to an increase in 3rd and 4th order terms such as trefoil (Z_3^{3}), vertical coma (Z_3^{-1}), and tetrafoil (Z_4^{4}). Surprisingly, spherical aberration values hardly changed after the cavity realignment.

The sources of these aberrations are mainly due to the optical elements within the cavity, such as lenses, mirrors, apertures, polarizers, and beam splitters. These contribute to produce different amounts of aberrations depending on their position, tilt, quality of surfaces, etc. For instance, lenses are usually made with spherical surfaces, which originate spherical aberration that increases with the beam size. If a beam entering the lens with some spherical aberration does not go along its optical axis, some coma is also produced. If the different conjugated optical planes along the laser pathway within the cavity are displaced to each other, some defocus might be produced. Amounts of nonsymmetric aberrations (astigmatism, trefoil,…) may be produced when the lenses are under tension or stress within the holder. A larger beam size is usually associated with an increase in aberrations since this propagates using a larger portion of the optical elements within the cavity. Defects on the surfaces of mirrors and beam splitters might also be responsible for different higher-order aberrations. Moreover, in our particular case, the noticeable reduction in astigmatism after the realignment process might also have its origin in the correction of the tilt of some lenses or mirrors.

On then other hand, the overall decrease in the amount of aberrations of the laser beam after the cavity alignment might be also due to an improvement in the spatial overlap of the two laser beams entering the amplifier cavity: the fs Mira laser and the Evolution pump laser. This ought to make aberrations smaller and more symmetric (defocus, spherical) with less of odd terms (such as coma, trefoil,…). It can be expected that if the two beam waists coincide axially better after the realignment, this would give higher power and presumably less total aberration.

The stability of the lower order aberrations here reported is not surprising, although to our knowledge not much work has been done on this topic [5]. An in-detail analysis of the temporal stability (before and after aligning the cavity) of high-power laser systems, including the behavior of higher-order aberrations as the one here presented, is lacking in the literature. In fact, we think that the temporal characterization of the WAs is the most important step before moving towards a possible compensation using adaptive optics.

The real-time measurement and monitoring of laser WAs might be helpful to optimize the beam quality while modifying the parameters within the laser cavity. Although this technique may be used as

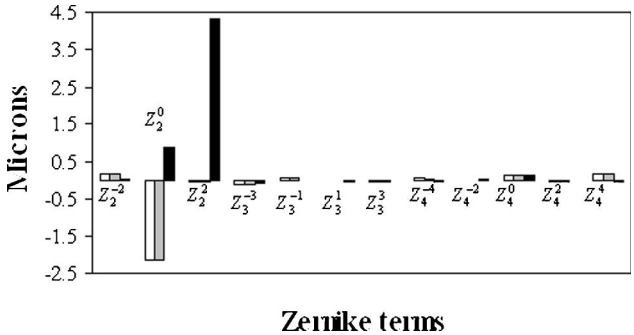

Fig. 10. Individual Zernike coefficient values of the WA (up to 4th order) for the high-power laser beam. White and gray bars correspond to the averaged values during 1 s and 1 h after the optics realignment. Black bars are the same as those in Fig. 4 (mean during 3 h).

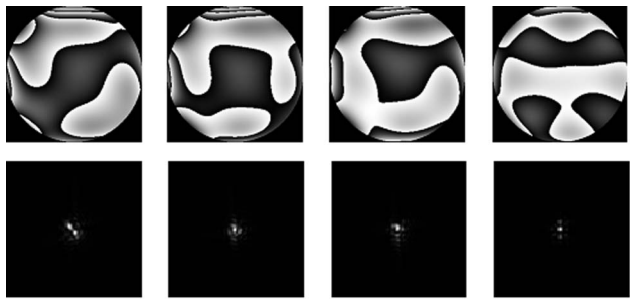

Fig. 11. WAs (upper row, 7 mm pupil) and PSFs (lower row, subtending 0.85°) corresponding to the predicted improvement in the quality of the high-power laser beam by removing different Zernike terms. Far left column: no defocus; second column from the left: no 2nd order terms; third column from the left: no 3rd order terms; far right column: no 4th order terms.

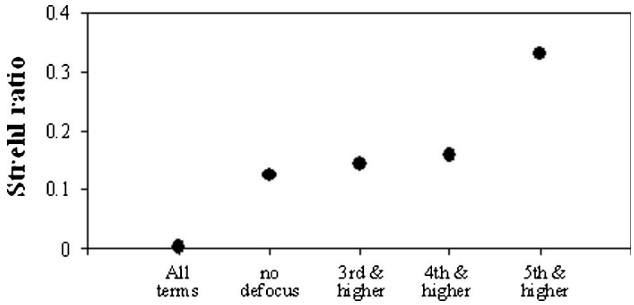

Fig. 12. Increase in the Strehl ratio of the PSF as a funtion of the corrected Zernike terms.

an alignment diagnostic tool, a cavity optimization cannot only be based on wavefront sensing since this operation not always guarantees a higher power. A rough power alignment must first be done, but once a satisfactory level of power has been reached additional adjustments are required (without sacrificing power) to ensure an improved laser beam quality with minimized aberrations has been reached. This is important to obtain a beam quality suitable (in space and time) for high-energy focusing.

Our results can be compared with some of the efforts by other groups that have reported studies on the WAs of high-power laser beams. Few experiments have been based on WA measurements at the output of a laser system obtained from HS sensing. Akaoka *et al.* [5] showed that before the correction using adaptive optics, astigmatism, defocus, and trefoil were the dominant terms. They provided values of about 0.7, 0.3, and 0.1 μm, respectively, without information on the pupil size used. Before correction they measured the WA during approximately 1.5 s. Although it seemed to be very stable, no analysis on this stability was done. More recently, Schäfer *et al.* characterized an ultrafast laser system by means of HS measurements [6,7]. Although they did not report data on temporal stability either, defocus was shown as the dominant term (two orders of magnitude higher than coma and three higher than spherical aberration).

However, most WAs measurements of high-power laser beams were carried out at different locations within large-facility laser research systems. In particular, measurements at the preamplifier in the Petawatt High-Energy Laser for Heavy-Ion Experiments (PHELIX, GSI Darmstadt) laser reported that the main aberrations were astigmatism and coma [17]. At the end of the PHELIX main amplifier, static aberrations were basically astigmatism (PtV = 0.27 μm) and spherical aberration (PtV = 0.42 μm). Pump-shot aberrations were mainly astigmatism (PtV = 0.2 μm) and coma (PtV = 0.1 μm). After a shot and during 3 h the long term aberrations were also analyzed. Both defocus and H-V astigmatism took maximum values just after the shot (PtV about 0.40 and 1.8 μm, respectively) [1]. Using a HS sensor placed at the end of a 100 TW Ti:sapphire chirped pulse amplification (CPA) laser [23], Planchon *et al.* showed that the most important aberrations were associated with lower order terms: 0.27 and 0.29 μm for H-V astigmatism and trefoil. Jeong *et al.* have also observed several monochromatic aberrations, such as astigmatisms, defocus, vertical coma, trefoils, and spherical aberration in a 100 TW Ti:sapphire laser beam [24]. Bahk *et al.* [25] measured the statistical RMS values of the wavefront using 10–20 shots of a CPA laser. The statistical RMS value, i.e., the shot-to-shot stability of the wavefront was found to be 0.06 μm. In a 100 TW Nd:glass, laser fluctuations of 0.032 μm in RMS (0.16 μm in PtV) were found in a 40 min period. These measurements used a three-wave lateral shearing interferometer as WA sensor [26].

Zou *et al.* have recently explored the contribution of static and thermal aberrations at the laser facility LULI2000 (Laboratoire pour l'Utilisation des Lasers Intenses) by means of a four-wave lateral shearing interferometer located at the end of the amplification chain [2]. For the former, PtV values of about 0.53 μm for static aberrations and values 10 smaller for total RMS were reported. These were thought to be originated by the fact that the beam axis does not perfectly coincide with the well-defined axes of the optical components (especially lenses). Since pump-shot aberrations were found to be much lower than thermal relaxation aberrations, these were measured during a 3 h recovery time after a full-energy kilojoule single shot. Defocus and astigmatism were the most important contributions. A strong H-V astigmatism was measured at the chain output as a result of a thermal cylindric lens generated in the amplifier disks. In particular, PtV values for individual Zernike terms associated with defocus varied from −0.12 to ∼0 μm, 45° astigmatism stayed at 0.12 μm, H-V astigmatism changed from −0.34 to −0.12 μm, and vertical coma values ranged between −0.05 and 0.03 μm.

In our case we used a commercially available laser system and, due to its special arrangement, a WA sensor outside the cavity. Although a direct comparison between data in the literature and those here presented cannot be done, our results are coherent with those previously published in the sense that we also found that 2nd order aberrations contribute the most to the total measured WA. Moreover, we measured the influence of a cavity realignment and found that this operation not only changed the magnitude of 2nd order aberrations but also higher-order terms. Differences between maximum and minimum values of PtV and RMS did not differ much between the two experiments, which means that those variations are not due to static aberrations but rather dynamic ones. Although the quality of the laser beam was improved, temporal stability was not affected. Comparing both temporal scales, the values for the Zernike coefficients hardly changed, which corroborates the stability also shown in Fig. 3.

The increasing number of applications of high-power light sources (high-energy-density physics

research, astrophysics laboratory experiments,…) are the basis for the continuous improvements in laser system performance. The laser beam WA limits the ability to obtain the desired high-quality focus and, therefore, to reach the energy density required for many experiments. Knowledge about the laser beam WA is the first step to producing well-focused and driven high-energy short pulses by subsequent wavefront correction using adaptive optics. Characterization of the temporal WA changes is important to test the benefit of both static and dynamic corrections.

The WA laser stability found here indicates an initial potential benefit with a static correction only. We have numerically studied the effects of correcting the different Zernike modes (Figs. 11 and 12). When removing the 2nd order terms (i.e., classical static correction) the RMS was reduced 85% (PSF Strehl ratio increased ~100 times). An additional reduction in the RMS of 20% (Strehl ratio increased 35%) is produced after correcting 3rd order terms. This correction would require an active corrector element, such as a deformable mirror.

To conclude, we built a real-time (25 Hz) HS sensor adapted to measure the temporal stability of ultrafast and high-power laser beams. Laser beam WAs were measured at two different temporal rates, before and after cavity realignment. Results show that the measured WA was fairly stable over time (changes lower than 1%). Defocus and astigmatism were the dominant aberration terms. We predicted how static correction by means of adaptive optics might improve the beam quality of the laser, leading to an improved ability for high-quality focusing. For higher intensity regimes, a larger temporal variability is expected and dynamic adaptive optics corrections might be required. Well-corrected beams could potentially provide near-diffraction-limited focal spots which are crucial in fields of research such as thermonuclear fusion and atomic and plasma physics, among others.

This work has been supported in part by the Ministerio de Educación y Ciencia of Spain, grants FIS2007-64765, CONSOLIDER-INGENIO 2010, CSD2007-00033 SAUUL; and the Fundación Seneca (Región de Murcia, Spain), grant 4524/GERM/06.

†Present address: School of Physics, University College Dublin, Dublin 4, Ireland.

References

1. H.-M. Heuck, U. Wittrock, J. Fils, S. Borneis, K. Witte, U. Eisenbart, D. Javorkova, V. Bagnoud, S. Götte, A. Tauschwitz, and E. Onkels, "Adaptive optics at the PHELIX laser," Proc. SPIE **6584**, 658402 (2007).
2. J.-P. Zou, A.-M. Sautivet, J. Fils, L. Martin, K. Abdeli, C. Sauteret, and B. Wattellier, "Optimization of the dynamic wavefront control of a pulsed kilojoule/nanosecond-petawatt laser facility," Appl. Opt. **47**, 704–710 (2008).
3. W. Koechner, "Thermal effect in laser rods," in *Solid-State Laser Engineering*, D. L. MacAdam, ed. (Springer-Verlag, 1976), pp. 365–382.
4. U. J. Greiner and H. H. Klingenberg, "Thermal lens correction of a diode-pumped Nd:YAG laser of high TEM00 power by an adjustable-curvature mirror," Opt. Lett. **19**, 1207–1209 (1994).
5. K. Akaoka, S. Harayama, K. Tei, Y. Maruyama, and T. Arisawa, "Close loop wavefront correction of Ti:sapphire chirped pulse amplification laser beam," Proc. SPIE **3265**, 219–225 (1998).
6. B. Schäfer, K. Mann, G. Marowsky, C. P. Hauri, J. Biegert, and U. Keller, "Characterization, wavefront reconstruction and propagation of ultra-broadband laser pulses from Hartmann–Shack measurements," Proc. SPIE **5918**, 59180P (2005).
7. B. Schäfer, M. Lübbecke, and K. Mann, "Propagation of laser beams from Hartmann–Shack measurements," Proc. SPIE **6343**, 634348 (2006).
8. A. Y. Kato, K. Mima, N. Miyanaga, S. Arinaga, Y. Kitagawa, M. Nakatsuka, and C. Yamanaka, "Random phasing of high-power lasers for uniform target acceleration and plasma instability suppression," Phys. Rev. Lett. **53**, 1057–1059 (1984).
9. J. Garnier, "Statistics of the hot spots of smoothed beams produced by random phase plates revisited," Phys. Plasmas **6**, 1601–1610 (1999).
10. R. Lehmberg and S. Obenschain, "Use of induced spatial incoherence for uniform illumination of laser fusion targets," Opt. Commun. **46**, 27–31 (1983).
11. D. Veron, G. Thiell, and C. Gouédard, "Optical smoothing of the high power PHEBUS Nd-glass laser using the multimode optical fiber technique," Opt. Commun. **97**, 259–271 (1993).
12. J. C. Chanteloup, F. Druon, M. Nantel, A. Maksimchuk, and G. Mourou, "Single-shot wavefront measurements of high-intensity ultrashort laser pulses with a three-wave interferometer," Opt. Lett. **23**, 621–623 (1998).
13. S. Matsuoka and K. Yamakawa, "Wavefront measurements of terawatt-class ultrashort laser pulses by the Fresnel phase-retrieval method," J. Opt. Soc. Am. B **17**, 663–667 (2000).
14. P. Yang, S. J. Hu, X. D. Yang, S. Q. Chen, W. Yang, X. Zhang, and B. Xu, "Test and analysis of the time and space characteristics of phase aberration in a diode-side-pumped Nd:YAG laser," Proc. SPIE **6018**, 182–191 (2005).
15. W. Lubeigt, G. Valentine, J. Girkin, E. Bente, and D. Burns, "Active transverse mode control and optimization of an all-solid-state laser using an intracavity adaptive-optic mirror," Opt. Express **10**, 550–555 (2002).
16. W. Lubeigt, P. van Grol, G. Valentine, and D. Burns, "Use of intracavity adaptive optics in solid-state laser operation at 1 μm," *Adaptive Optics for Industry and Medicine: Proceedings of the 4th International Workshop*, Vol. 102 (Springer, 2005), pp. 217–227.
17. H.-M. Heuck, U. Wittrock, C. Häfner, S. Borneis, E. Gaul, T. Kühl, and P. Wiewior, "Wavefront measurement and adaptive optics at the PHELIX laser," *Adaptive Optics for Industry and Medicine: Proceedings of the 4th International Workshop*, Vol. 102 (Springer, 2005), pp. 283–290.
18. W. Lubeigt, G. Valentine, and D. Burns, "Enhancement of laser performance using an intracavity deformable membrane mirror," Opt. Express **16**, 10943–10955 (2008).
19. I. Ghozeil, "Hartmann and other screen tests," in *Optical Shop Testing*, D. Malacara, ed. (Wiley, 1992), pp. 367–396.
20. P. M. Prieto, F. Vargas, S. Goelz, and P. Artal, "Analysis of the performance of the Hartmann–Shack sensor in the human eye," J. Opt. Soc. Am. A **17**, 1388–1398 (2000).
21. J. C. Wyant and K. Creath, "Basic wavefront aberration theory for optical metrology," in *Applied Optics and Optical Engineering*, B. Shannon and J. C. Wyant, ed. (Academic, 1992), Chap. 1, Vol. XI, pp. 1–39.

22. J. Lee, R. V. Shack, and M. R. Descour, "Sorting method to extend the dynamic range of the Shack–Hartmann wavefront sensor," Appl. Opt. **44**, 4838–4845 (2005).
23. T. A. Planchon, J.-P. Rousseau, F. Burgy, G. Chériaux and J.-P. Chambaret, "Adaptive wavefront correction on a 100 TW/10 Hz chirped pulse amplification laser and effect of residual wavefront on beam propagation," Opt. Commun. **252**, 222–228 (2005).
24. T. M. Jeong, W. Choi, N. Hafz, J. H. Sung, S. K. Lee, D.-K. Ko, and J. Lee, "Wavefront correction and customization of focal spot of 100 TW Ti:sapphire laser system," Jpn. J. Appl. Phys. **46**, 7724–7730 (2007).
25. S.-W. Bahk, P. Rousseau, T. A. Planchon, V. Chvykov, G. Kalintchenko, A. Maksimchuk, G. A. Mourou and V. Yanovsky, "Generation and characterization of the highest laser intensities (1022 W/cm2)," Opt. Lett. **29**, 2837–2839 (2004).
26. B. Wattellier, J. Fuchs, J-P. Zou, K. Abdeli, H. Pépin and C. Haefner, "Repetition rate increase and diffraction limited focal spots for a nonthermal-equilibrium 100 TW Nd:glass laser chain by use of adaptive optics," Opt. Lett. **29**, 2494–2496 (2004).